March - April 2020
ISSN: 0193-4120 Page No. 7222 - 7234

Effect of Friction Stir Processing on Microstructure and Mechanical Properties of TIG Welded Aluminum Alloy 2024-T3

Muna Khethier Abbass* Jihad Ghanim Abdulkader**
Dept. of Production Engineering and Metallurgy, University of Technology,

Baghdad-Iraq

* Email:mukeab2014@yahoo.com ** jihad82eng@yahoo.com

Article Info
Volume 83
Page Number: 7222 - 7234
Publication Issue:
March - April 2020

Article History
***Article Received**: 24 July 2019*
***Revised**: 12 September 2019*
***Accepted**: 15 February 2020*
***Publication**: 06 April 2020*

Abstract
This present work aims to demonstrate the effect of friction stir processing (FSP) on the microstructure and mechanical properties of TIG welded joints of aluminum alloy AA2024-T3 with using ER4047 filler metal. The welded specimens were exposed to tensile and hardness tests and microstructure assessment at the best FSP parameters (1000 rpm and 16 mm/min). Tensile strength for TIG +FSP joint was (317MPa) that showed higher value than that of TIG weld (225 MPa), hence showing 41% increase from TIG weld. Also the hardness values of TIG + FSP specimen comes out to be 137-141HV which were higher than the base metal (124HV), whereas in TIG specimen hardness values were 115-118HV. That means there is improvement in the hardness value. Optical microscopic analysis has been done on the weld joint to evaluate the effect of FSP parameters on welding quality and microstructure. Microstructure of TIG + FSP joint sample is very fine equiaxed grains in stir zone of FSP which is better than the microstructure of TIG joint which is column grains in weld zone.

Keywords: TIG welding , aluminum alloys (AA2024-T3), friction stir processing, microstructure, mechanical properties.

1-Inroduction

Aluminum alloys are important for fabrication of segments and structures which require high strength to low weight properties have generous thought in aerospace, automotive industries, ship building and cryogenic application to enhance the fuel efficiency in transportation industry and moderate the ecological issues [1-2]. However, the joining of aluminum alloys unremittingly meant an incredible test for assembling engineers. Specifically, the heat treatable aluminum alloys such as 2024 alloy and its combination to other materials is difficult to fabricate using conventional fusion welding

March - April 2020
ISSN: 0193-4120 Page No. 7222 - 7234

methods [3-4]. The weldments after fusion welding resulted in formation of some welding defects like porosity, micro cracks in fusion zone during the weld pool solidification from the molten state to solid state. Also, there are lots of different difficulties are consorted to this type of joining methods, specifically these are associated with presence of persistent oxide layer, solidification shrinkage, thermal expansion, high thermal conductivity and high solubility of hydrogen and different gases in the weld pool [5-6].

There are few techniques applied for example heat treatment processes, tungsten inert gas welding (TIG) that the dissolving and mechanical twisting process are occurred to modify the materials properties so as to improve the joint properties. In any case, these techniques are not productive and a portion of those are not pertinent for using welded joints, where the joint quality is highly required. Most as of late, (FSW) become a conspicuous welding process for joining of aluminum alloys, which was invented by The Welding Institute (TWI) in 1991 [7-8]. Moreover, it is also suitable for joining of dissimilar materials like friction welding, diffusion bonding and roll bonding processes [9-10].

FSW technique includes a cylindrical rotating tool of non-consumable type material that plunges into the two sheets and moves between the butt crease, stirs, and reinforced them together without softening of the welded metal. The further upgrades in FSW process later years resulted in development of a friction stir processing procedure. FSP is additionally similar to a FSW process that can produce an extreme plastic deformation in the weldments and utilized as an aggregate tool for the surface and microstructural adjustments of different materials and aluminum alloys [11]. FSP has several advantages over the other metal working processes, such as improving the microstructural formation by refining the grain size, its densification and homogeneity of gain distribution in a single pass. The microstructures and mechanical properties of the weld metals can be easily controllable by adjusting or optimizing of process conditions and FSP is efficient technique for surface modifications [12]. In particular, FSP of the as-cast alloys exhibits a wide range of grain refinement, destroying and dissolution of the precipitates and avoid the porosity in the weldments; thereby it putting up an appealing ductility, strength and crack free weld microstructures.

Many researchers studied the effect of FSW and FSP individually on mechanical properties of aluminum alloys but limited researches focused on TIG welding followed by FSP and its effects on the mechanical properties and microstructure observation. **Robin Thakral *et al.*** [13] in 2018 made experimental analysis of FSP of TIG welded aluminum alloy 6061 and they concluded that the tensile strength of TIG welded joint was (85 MPa) and 125Mpa for TIG+FSP joint, hence showing 48% increase from the TIG welded joint. **Krishnaja Devireddy *et al.***[14] applied a new technique of both GTAW+ FSP to the 2024 aluminum alloy plate of 5mm thickness to improve the weld metal properties. The filler metal was

March - April 2020
ISSN: 0193-4120 Page No. 7222 - 7234

ER5356 with a diameter of 2.4 mm for filling the butt joint. The results demonstrated that the FSP over GTAW welds modified the microstructure and mechanical properties of GTAW welds. **Muna K. Abbass and Noor B. Shurhan** [15] in 2019 utilized Taguchi method and design of experiment to optimize the friction stir processing parameters depending on tensile strength of aluminum alloy AA 6061-T6. FSP was achieved under three different rotation speeds (800, 1000 & 1250 rpm) and travel speeds (16, 25& 32mm/min) and number of passes (1, 2 &3). It was found that the best FSP parameters were 1250 rpm and 32 mm/min and two passes.

Welding of aluminum poses a great challenge to get a sound proof joint as many problems are encountered during the welding , it was decided to weld the 2024-T3 aluminum alloy with different welding processes viz. Tungsten Inert Gas Welding (TIG) & Friction Stir Processing (FSP). The aim of present work is used a novel approach for AA2024-T3 aluminum alloy of TIG welded joint by applying FSP procedure to enhance the microstructural development and mechanical properties.

2-Experimental Work

The heat-treated AA2024-T3 aluminum alloy used in the present investigation is in the form of sheet 3.2mm thickness, samples were prepared by cutting machine into 18 pieces with the dimensions of 150 x 50 x 3.2 mm. Its chemical composition is shown in **Table 1,** also filler metal type (ER4047) was used, its chemical composition is shown in **Table 2.**

Table 1: Nominal and measured chemical composition of aluminum alloy AA2024-T3

Element Wt%	Cu	Mg	Fe	Mn	Si	Zn	Cr	Ti	Pb	V	AL
Nominal (value)[17]	3.8min. 4.9max.	1.2min. 1.8max.	0.5 max.	0.3min. 0.9max.	0.5 max.	0.25 max.	0.1 max.	0.15 max.	0.05 max.	0.05 max.	Balance
Measured Value	4.25	1.27	0.334	0.050	0.157	0.454	0.002	0.001	0.024	0.009	Balance

Table 2: Nominal and measured chemical composition of the filler wire ER4047

Element Wt%	Mg	Mn	Si	Zn	Fe	Cu	Be	Al
Nominal (value)[17]	0.10 % max.	0.15 % max.	11.0-13.0 %	0.20 % max.	0.8% max.	0.30 % max.	0.0008 % max.	Balance
Measured Value	0.022	0.001	12.0	0.20	0.15	0.005	0.008	Balance

The sheets were cleaned with acetone to remove the oil, dirt etc., and are brushed with steel wire brush to evacuate the oxide layer, before to the TIG welding, samples cleaned with alcohol and dried to remove the moisture in the sheets. After removal of the oxide layer, edge preparation was done for making the butt joint and spaced

March - April 2020
ISSN: 0193-4120 Page No. 7222 - 7234

by a gap about (2mm) to allow molten filler metal to diffuse, Welding parameters of TIG welding as shown in the **Table 3.**

Table 3: Details of TIG welding used in this study

Weld characteristic	Weld detail
Material type	AA2024-T3
Joint type	Butt weld
Sample dimensions	150 ×50×3.2mm^3
Tungsten electrode Rod type	Pure tungsten(EWP)
Tungsten electrode dimension	2.4 mm
Cup Size	10 mm
Filler type	ER4047
Filler rod dimension	2mm
Polarity	Alternating Current(AC high frequency)
Amperes Range (A)	115A
Voltage (V)	13.5V
Frequency	100hz or greater
Shielding gas	Argon
Gas composition	99.99999
Argon shielding gas	8L/min.
Gas flow rate	17cfh or 20psi
Post welding Gas Flow Time	10sec.
AC Balance	Balance wave(50%Electrode positive-50%Electrode Negative)
Welding speed	12inches per minute
Backing Tape type	(CBT-CG)Ceramic Backing Tape – Curved Groove
TIG Setup	Manual

FSP tool was made of X12M steel and consists of a shoulder and concentric pin. The shoulder diameter of the tool is 18 mm and the pin of the non-consumable tool was threaded cylindrical (TCY) , diameter of pin is 6mm and length of pin is 3 mm , and it was heat-treated to enhance the hardness properties as shown in the **Table 4.**

Table 4: Details of friction stir processing used in this study

March - April 2020
ISSN: 0193-4120 Page No. 7222 - 7234

Parameters	Processing detail
Rotational speed	1000 rpm
Travel speed	16 mm/min
Tool type	TCY
Shoulder diameter	18mm
Pin diameter	6mm
Pin length	3mm
hardness of tool	53-55 HRc

Two sets of samples were made first was TIG welded only and second was TIG welded followed by FSP (TIG +FSP joint sample) are shown in **Figure 1**. These two sets of specimens (TIG welded joint and TIG+FSP joint) were cut across the weld seams, and are prepared for the microstructural characterization as per the standard metallographic procedures. To reveal the microstructural features, polished samples were etched with Killer's reagent (components : 95ml H_2O , 2.5ml HNO_3, 1.5ml HCl, 1.0ml HF) and afterward cleaned by water,alcohol and then dried it in oven for better visibility of the microstructures. The microstructural analysis was completed by optical microscope , and the Vicker's micro hardness tester has been used for hardness measurements across the cross section of the welds, In agreement to ASTM,micro hardness tests were performed at the situations on the two sides of TIG welded joint and processed joint,the reading was taken for each 1 mm distance. A 200g load was applied to cross section of the TIG welded joint and processed joint for (15) second. The ASTM E8 standard was used for preparing the tensile samples. All the samples were tested at room temperature using crosshead speed of 0.5 mm/min to obtain the reliable strengths.

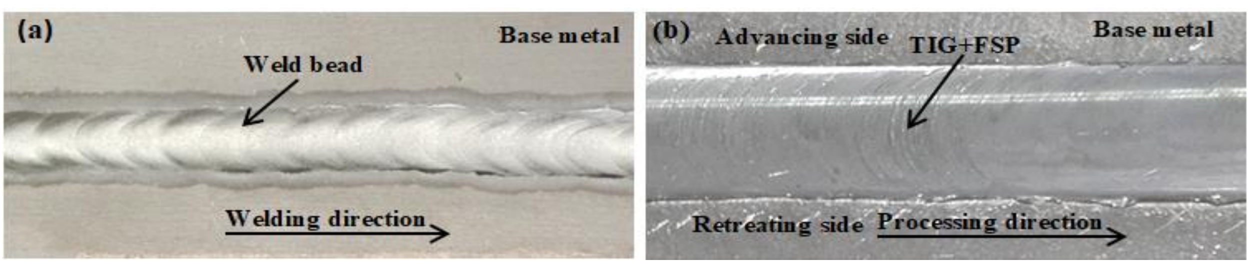

Figure 1: Macro graphs of the (a) TIG welded sample and (b) TIG + FSP Joint processed sample

3-Results and Discussion

3.1 Micro-structure

Microstructures of base metal and TIG welded specimen at the cross section of the joint and the microstructure of TIG +FSP joint samples were taken by using an optical microscope at 100x magnification after proper grinding and polishing and etching. Microstructure of base metal (AA2024-T3) is shown in **Figure 2.**

Figure 3 (a & b) shows the microstructures of TIG welded joint (with using ER4047 filler metal) which consists three zone , metal weld zone (WZ) , heated affected zone (HAZ) and unaffected zone (BM) .The microstructures of TIG weld + FSP joint specimen is shown in **Figure 4(a,b &c).** The optical micrographs of the weld metal with using filler ER4047 and the HAZ and unaffected zone of TIG welded joint specimens are shown in **Figure 3.** The structure increasingly coarser and column near HAZ for TIG welded joint**.** It can be observed that the grain structure was small column and was fineaxed at the weld metal or pool. disengagements that has high density with network structure observed in many grains and porosity and cracks were observed and because of that the tensile strength of TIG welded joint was less than that of base alloy (455 MPa).

The optical micrograph of TIG weld followed by the friction stir processing (TIG+FSP) joint is shown in **Figure 4**. The friction stir processing over TIG weld leads to formation four zone, stir zone (SZ), thermo-mechanical affected zone (TMAZ), HAZ and unaffected zone (BM). This hot deformation by FSP leads to the formation of extremely fine equiaxed recrystallized grains with in the friction stir zone processed. Different disengagements with network structure observed in the recrystallized grains. A high density of dislocations with network structure observed in many grains. Subsequently, the tensile test properties of FSP joint is better as compared to TIG welded joint due to thermo mechanical processing occurring through friction stir processing.

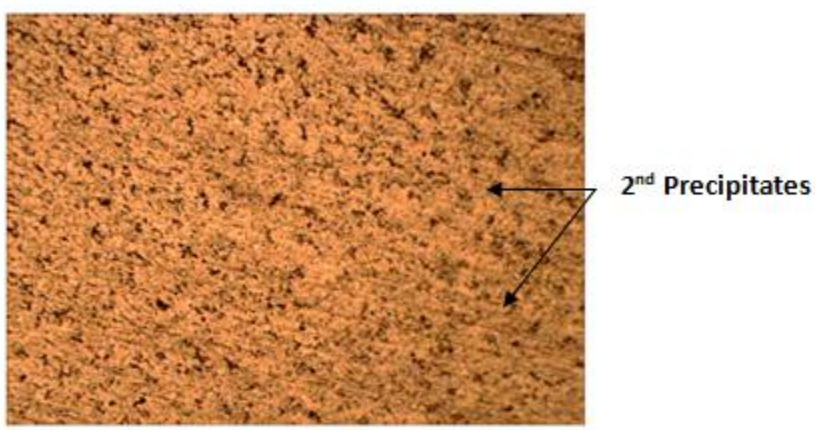

Figure 2:
Microstructure of base alloy AA2024-T3 at 100X

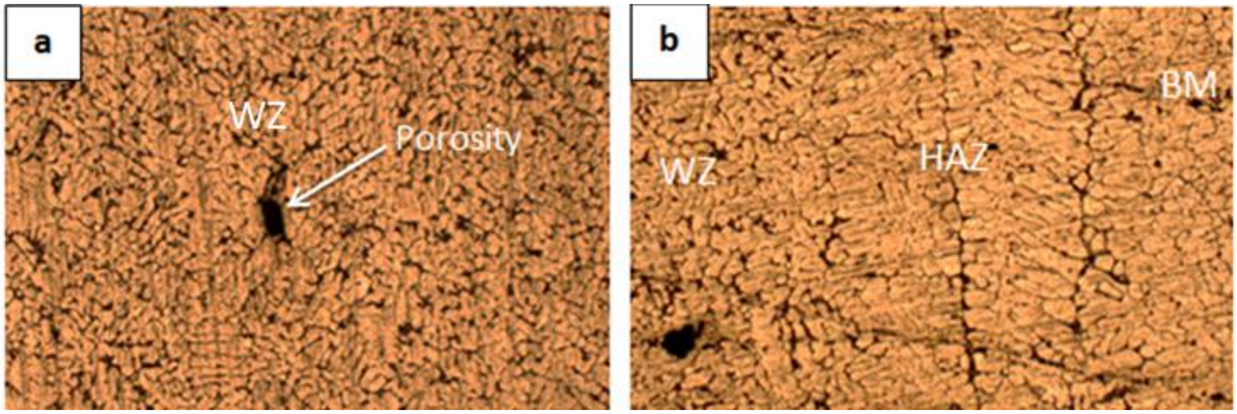

Figure 3: Microstructure of TIG welded joint (a) weld metal zone (WZ), (b) HAZ and unaffected zone (BM).at 100X

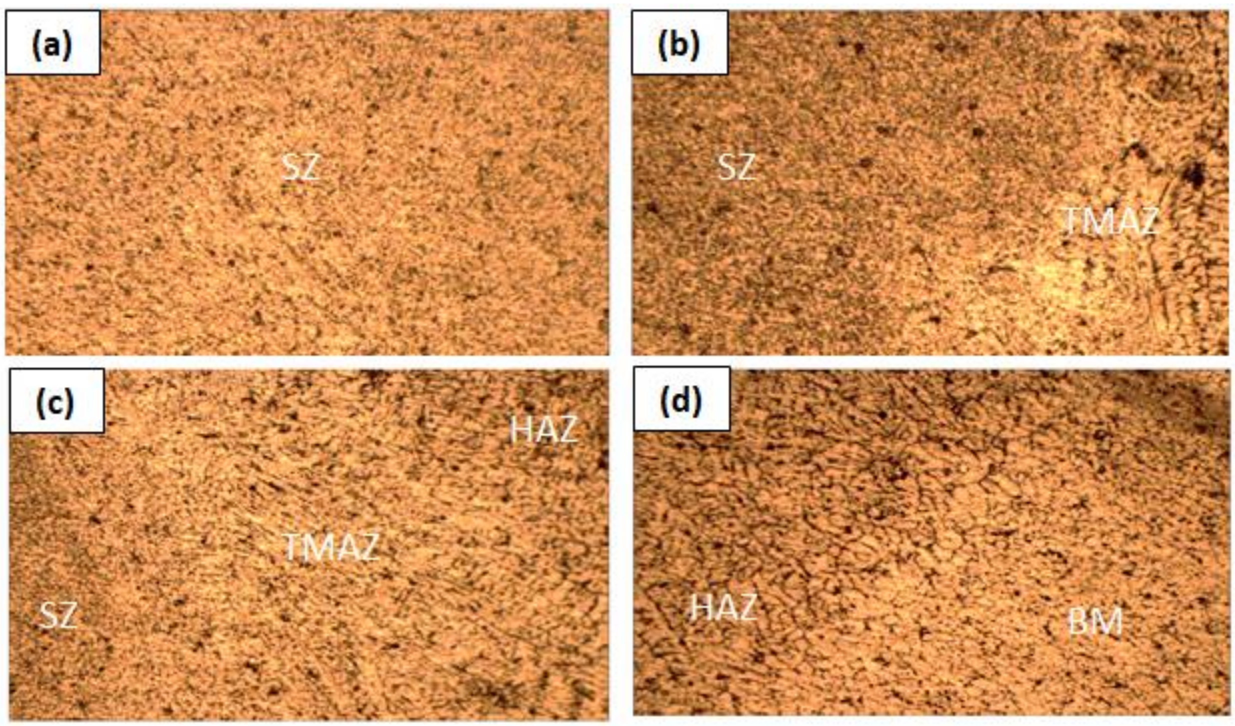

Figure 4: Microstructures of the TIG +FSP joint specimen at 100X.

3.2 XRD Analysis

XRD analysis was performed utilizing X-Ray diffract meter type (Shimadzu - XRD-6000) Japan utilizing Cu-tube with wavelength 1.540 A°,current 30 mA,voltage 40KV and scan rate was 5° / min to identify the main phases in the base alloy and weld.

XRD analysis was carried out in the base alloy AA2024-T3 and TIG welded joint with utilizing (ER4047 filler metal) at the best conditions as shown in Figures 5 and 6 respectively.It was observed the presence of 2nd phase precipitates of Al2Cu (?) and Al2CuMg (S) distributed homogenously in Al-matrix.The formation of those phases could improve the strengthening effect as well to the particulate reinforcement in the stir zone[17].

The combinated effect of temperature and plastic deformation during FSP over TIG welded joint caused refined grains in stir zone and the large precipitates particles of the base alloy,also the large Si-particles in weld zone to be broken and fragmented into fine particles and distributed homogenously in Al-matrix. These results are confirmed by many researchers [18,19].

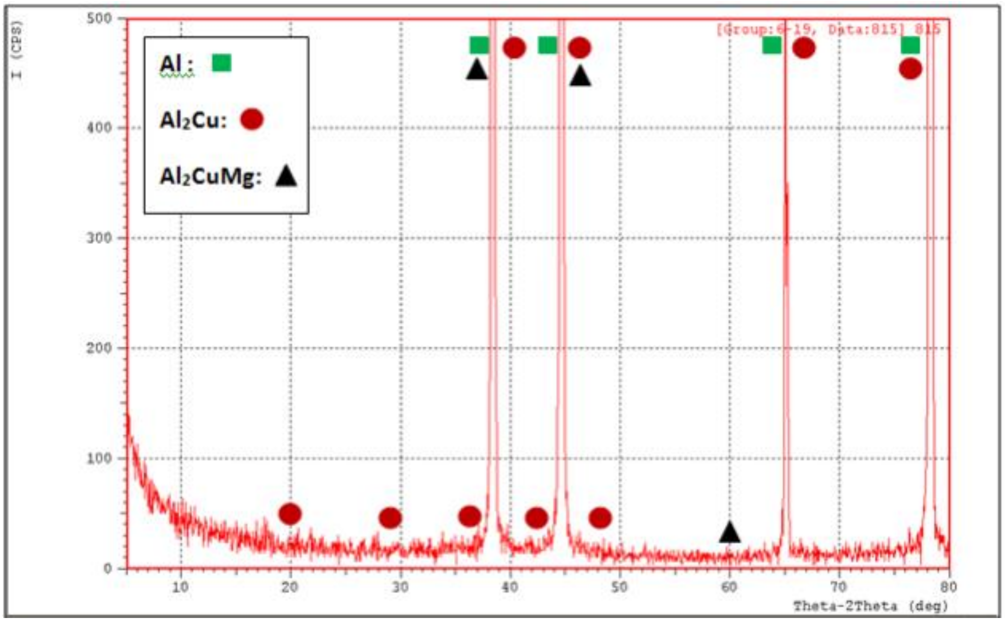

Figure 5: XRD analysis for base alloy AA2024- T3

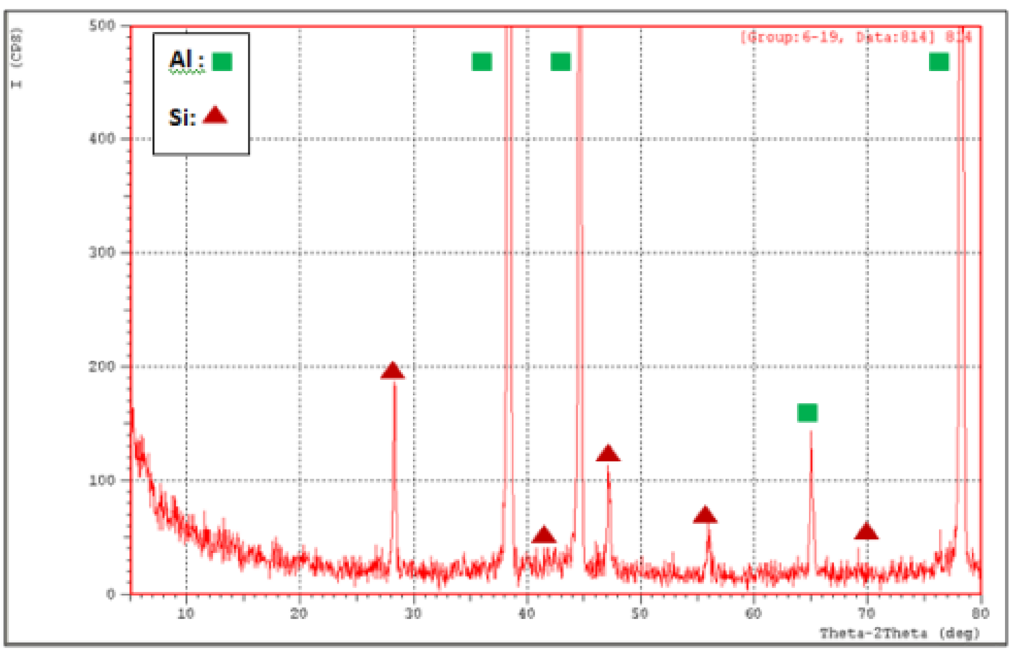

Figure 6: XRD for TIG welded joint with using ER4047 filler metal for AA2024- T3

March - April 2020
ISSN: 0193-4120 Page No. 7222 - 7234

3.3 Tensile Test

Tensile test was performed on universal testing machine of WDW-200E model with maximum load capacity 600 KN. Maximum tensile strength was found from the stress strain curve as shown in **Figure 7. Table 5** shows the mechanical properties which represent the tensile strengths values for the base alloy (AA2024-T3),welded joint produced by TIG welding and TIG+FSP joint specimen. hence showing TIG+FSP joint specimen41% increase from TIG welded joint. The joint efficiency for welded specimen by TIG was 50% and TIG +FSP specimen was 70% as compared with the base alloy.

The results of the TIG welds consisting of porosity and micro cracks in the fusion zone, which are causes to impair the mechanical properties of the welds. In order to overcome the defects, FSP procedure was applied along the TIG weld bead up to all depth of the weld zone from the top surface of the welds. The resultant welds were studied in detail to characterize the microstructural differences, grain growth and porosity defects. Furthermore, the effect of FSP procedure on the mechanical properties of the welds was evaluated, and is compared with the newly formed FSP microstructural zones to understand and improve the weld metal characteristics. Karthikeyan and Senthil Kumar [20] explained in details these enhancement in mechanical properties.They indicated that during FSP,severe plastic deformation and thermal exposure of alloy or material results in a significant evolution of the local microstructure,also eliminates internal defects in the material being processed and thereby improves its tensile strength ,ductility and other properties.

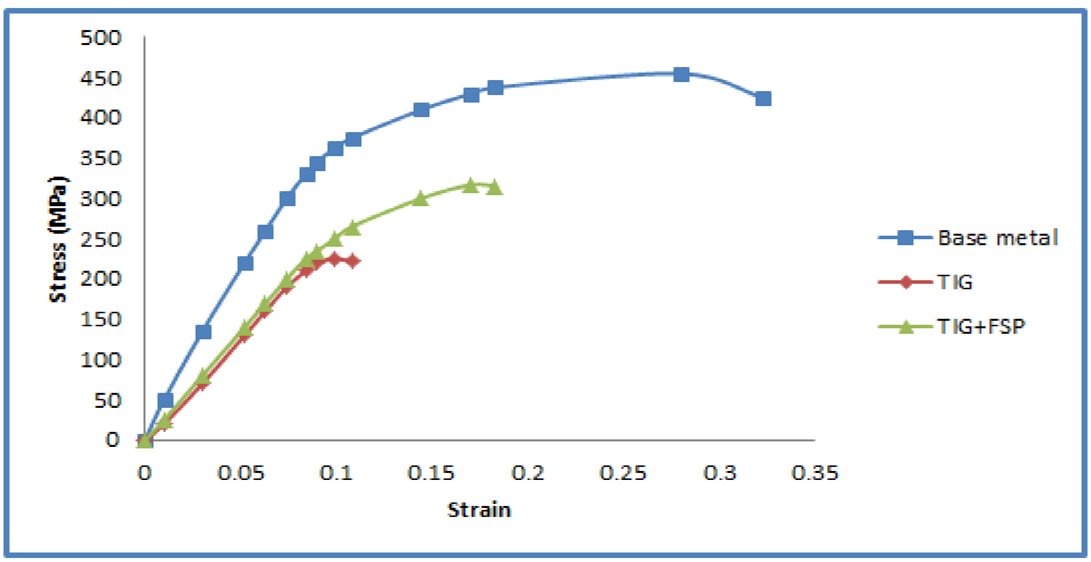

Figure 7: Stress-strain curves of base alloy (AA2042-T3), TIG welded joint and (TIG +FSP) joint specimen at the best conditions (1000 rpm and 16 mm/min).

Table 5:Shows Mechanical Properties for the base alloy AA2024- T3, TIG welded joint and TIG+FSP Specimen.

Materials	Yield strength YS(MPa)	Ultimate Tensile strength UTS(MPa)	Elongation %
Base alloy AA2024-T3 Standard value	345	480	18
Base alloy AA2024-T3 Measured value	340	455	21
TIG weld with ER4047	100	225	7
TIG weld +FSP	98	317	12

3.4 Micro-Hardness

The Vickers hardness test (HV) was carried out by utilizing digital micro-hardness tester, hardness measurements were performed on cross section at the positions on two sides TIG welded specimen and processed specimen.

Figure 6 shows the hardness distribution values (HV) of test specimen from the center to the heat affected zone (HAZ). The average hardness value of the base metal was 124 HV. The hardness value of TIG welded joint at the weld metal was 115-118 HV and at the heat affected zone (HAZ) was 90-103 whereas the hardness value of TIG + FSP joint specimen at the stir zone was 137-141 HV.The minimum hardness value was found in HAZ for TIG welded and TIG+FSP joints and begin to increase slightly through the TMAZ for both the advancing and retreating side toward the stir zone. The hardness of the TIG+ FSP joint in stir zone was the higher than other zones and base alloy. This is due to formation of very fine re-crystallized grains in the stir zone. These outcomes are in agreement with researchers [16, 17] in their studies when they used friction stir welding (FSW) for the similar and dissimilar aluminum alloys.

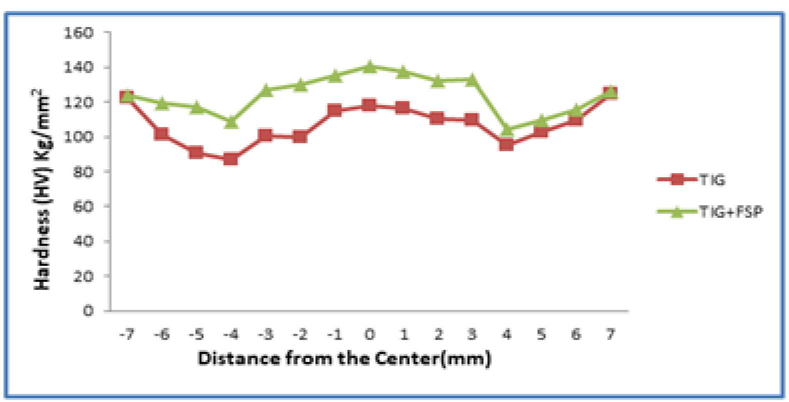

Figure 6: Micro hardness distribution across section of TIG weld and (TIG +FSP) joint samples at the best conditions (1000 rpm and 16 mm/min).

March - April 2020
ISSN: 0193-4120 Page No. 7222 - 7234

3.5 Fracture Surface Analysis

Scanning electron microscope (SEM) was used to study the characterization of the fracture surface morphologies for TIG welded specimen and TIG+FSP specimen after tensile test as shown in Figure 9 (a&b). the equiaxed dimples and hemispherical micro- voids were observed on the fractured surface. The dimple is a main feature of the fracture surface. Its size, shape and distribution are strongly depending on the nucleation, growth and coalescence of the micro voids during fracture. The dimples on the fracture surface of the TIG sample are large and deep, as shown in Figure 9a. This indicated that the ductile failure occurred in the welded joint of TIG specimen under tensile loading. Figure 9b depicts that the fracture surface contains small and shallow dimples with a waved and fibrous structure.and therefore, the size and depth of dimple decrease with the effect (FSP) .This is due to the plastic deformation and frictional heat during FSP, which leads to formation of micro cracks formed inside the structure of alloy and grew under the tensile stress, which can finally result in the fracture.

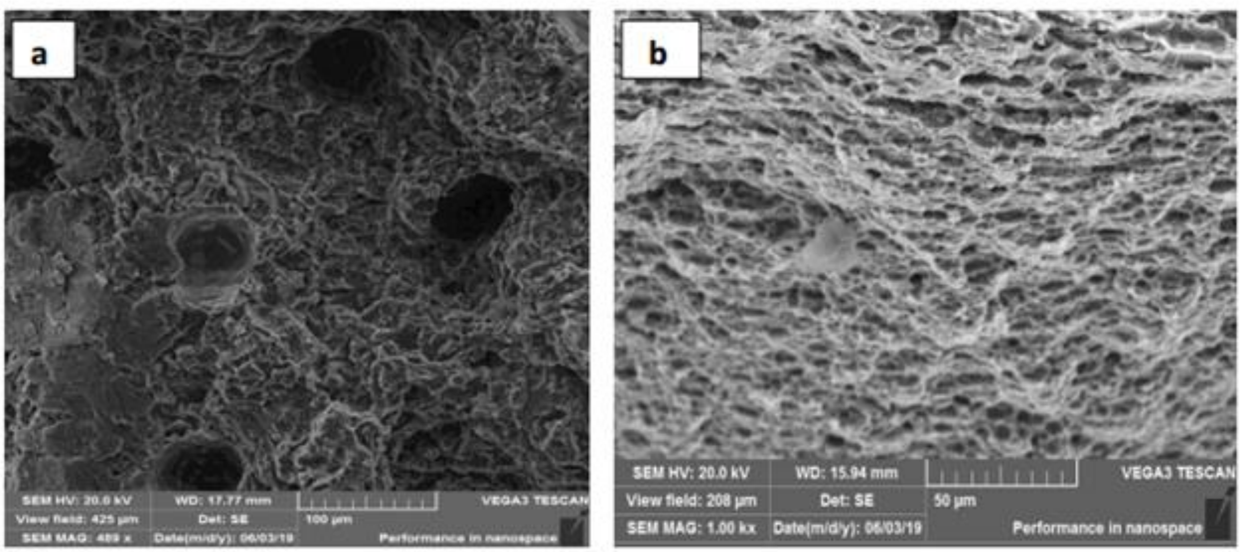

Figure 9: SEM micrographs of fracture surface after tensile test for TIG welded joint (a) and (b) for TIG + FSP joint at the best the conditions (1000 rpm and 16 mm/min)

4- Conclusions

1. TIG weld process + FSP procedure are new method was effectively applied to the aluminum alloy AA2024-T3 to improve the weld joint properties.
2. The defects and porosities formed in the TIG weld are reduced by using FSP process. The joint efficiencies for TIG welded joint (with using filler metal ER4047) and TIG + FSP joint were 50% and 70% respectively

March - April 2020
ISSN: 0193-4120 Page No. 7222 - 7234

as compared to strength of base alloy.

3. The FSP over the TIG weld fully modified the micro structure and improved the mechanical properties of the TIG welded joint. There is an 41% increase in tensile strength from TIG welded joint.
4. The micro hardness test for TIG+FSP joint specimen was higher than the micro hardness test for TIG welded joint because to formation of fine grain structure in the stir zone of TIG+FSP joint .
5. The FSP has broken the precipitates and Si particles and filled the gas pores by its stirring effect during FSP process resulted in enhancing of weld metal characteristics, strength and ductility of the joints.

References

1. Venkateswarlu, D., Rao, P. N., Mahapatra, M. M., Harsha, S. P., and Mandal, N. R. (2015). Processing and optimization of dissimilar friction stir welding of AA 2219 and AA 7039 alloys. Journal of Materials Engineering and Performance, 24(12), (2015) 4809-4824.
2. Cavaliere, P., Santis, A. D., Panella, F., and Squillace, A. (2009) " Effect of welding parameters on mechanical and microstructural properties of dissimilar AA6082–AA2024 joints produced by friction stir welding", Materials and Design, 30, 609-616.
3. Yigezu, B. S., Venkateswarlu, D., Mahapatra, M. M., Jha, P. K., and Mandal, N. R. "On friction stir butt welding of Al +12Si/10 wt% TiC in situ composite", Materials and Design, 54 (2014)1019-1027.
4. Aydın, H., Bayram, A., Uguz, A., and Akay, K. S. "Tensile properties of friction stir welded joints of 2024 aluminum alloys in different heat-treated-state", Materials and Design, 30(2009) 2211-2221.
5. Muralimohan, C. H., Haribabu, S., Reddy, Y. H., Muthupandi, V., and Sivaprasad, K. "Joining of AISI 1040 steel to 6082-T6 aluminium alloy by friction welding". Journal of Advances in Mechanical Engineering and Science, 1(1),(2015) 57-64.
6. Matrukanitz, R. P. "Selection and Weldability of Heat-Treatable Aluminum Alloys", ASM Handbook-Welding, Brazing and Soldering, Ohio: ASM International, 1990.
7. Mohanty, H. K., Venkateswarlu, D., Mahapatra, M. M., Kumar, P., and Mandal, N. R. " Modelling the effects of tool probe geometries and process parameters on friction stirred aluminium welds", Journal of Mechanical Engineering and Automation, 2(4), (2012)74-79.
8. Thomas, W. M., Nicholas, E. D., Needham, J. C., Murch, Temple-Smith, M.G.P.,and Dawes C.J. "International Patent Application" PCT/GB92/02203 and GB Patent

Application 9125978.8, London, 1990.
9. Venkateswarulu, D., Cheepu, M., Krishnaja, D., and Muthukumaran, S. (2018). Influence of Water Cooling and Post-Weld Ageing on Mechanical and Microstructural Properties of the Friction-Stir Welded 6061 Aluminium Alloy Joints. Applied Mechanics and Materials, 877, (2018) 163-176.
10. Cheepu, M., Ashfaq, M., and Muthupandi, V., "A new approach for using interlayer and analysis of the friction welding of titanium to stainless steel", Transactions of the Indian Institute of Metals, 70, (2017) 2591-2600.
11. Cheepu, M., Haribabu, S., Ramachandraiah, T., Srinivas, B., Venkateswarulu, D., Karna, S., Alapati, S., and Che, W. S. ,"Fabrication and Analysis of Accumulative Roll Bonding Process between Magnesium and Aluminum Multi-Layers, Applied Mechanics and Materials, 877, (2018) 183-189.
12. Mishra, R. S., and Mahoney, M. W. " Friction Stir Welding and Processing", Ohio: ASM International ,2007.
13. Robin Thakral and Sanjeev Sharma , Taljeet Singh, " Experimental analysis of friction stir processing of TIG welded aluminum alloy 6061" ,International Journal for Innovative Research in Science & Technology (IJIRST), 4(8), (2018) 51-57.
14. Krishnaja Devireddy, Venkatesw Arlu Devuri Muralimohan Cheepu and B. Kranthi Kumar ," Analysis of the influence of friction stir processing on gas tungsten arc welding of 2024 aluminum alloy weld zone", International Journal of Mechanical and Production Engineering Research and Development (IJMPERD) ,TJPRC Pvt.Ltd, 8(1), (2018) 243-251.
15. Muna K. Abbass, Noor Alhuda B. Sharhan ," Optimization of friction stir processing

parameters for aluminum alloy (AA6061-T6) using Taguchi method", Al-Qadisiyah Journal for Engineering Sciences, 12 (2019) 1-6.
16. Muna K. Abbass, Hassan H. Abd, A Comparison Study of Mechanical Properties between Friction StirWelding and TIG Welded Joints of Aluminum Alloy (Al 6061-T6), Engineering and Technology Journal, 31(14 Part (A) , (2013) 2701-2715.
17. Muna Khethier Abbass, Sabah Khamass Hussein & Ahmed Adnan Khudhair, Optimization of Mechanical Properties of Friction Stir Spot Welded Joints for Dissimilar Aluminum Alloys (AA2024-T3 and AA 5754-H114), AJSE.Arabian" Journal of Science and Engineering. 41(11), (2016) 4563-4572.